Structural basis of protection against H7N9 influenza virus by human anti-N9 neuraminidase antibodies

Xueyong Zhu[1#], Hannah L. Turner[1#], Shanshan Lang[1], Ryan McBride[2], Sandhya Bangaru[3], Iuliia M. Gilchuk[3], Wenli Yu[1], James C. Paulson[2], James E. Crowe, Jr.[3,4,5], Andrew B. Ward[1*], Ian A. Wilson[1,6*]

[1]Department of Integrative Structural and Computational Biology, The Scripps Research Institute, La Jolla, CA 92037, USA.

[2]Departments of Molecular Medicine, and Immunology and Microbiology, The Scripps Research Institute, La Jolla, CA, 92037, USA.

[3]Vanderbilt Vaccine Center, Vanderbilt University Medical Center, Nashville, TN, 37232, USA.

[4]Department of Pathology, Microbiology and Immunology, Vanderbilt, University Medical Center, Nashville, TN, 37232, USA.

[5]Department of Pediatrics, Vanderbilt University Medical Center, Nashville, TN, 37232, USA.

[6]Skaggs Institute for Chemical Biology, The Scripps Research Institute, La Jolla, CA, 92037, USA

[#] These authors contributed equally to this work.

[*] Correspondence: wilson@scripps.edu (I.A.W.); andrew@scripps.edu (A.B.W.)

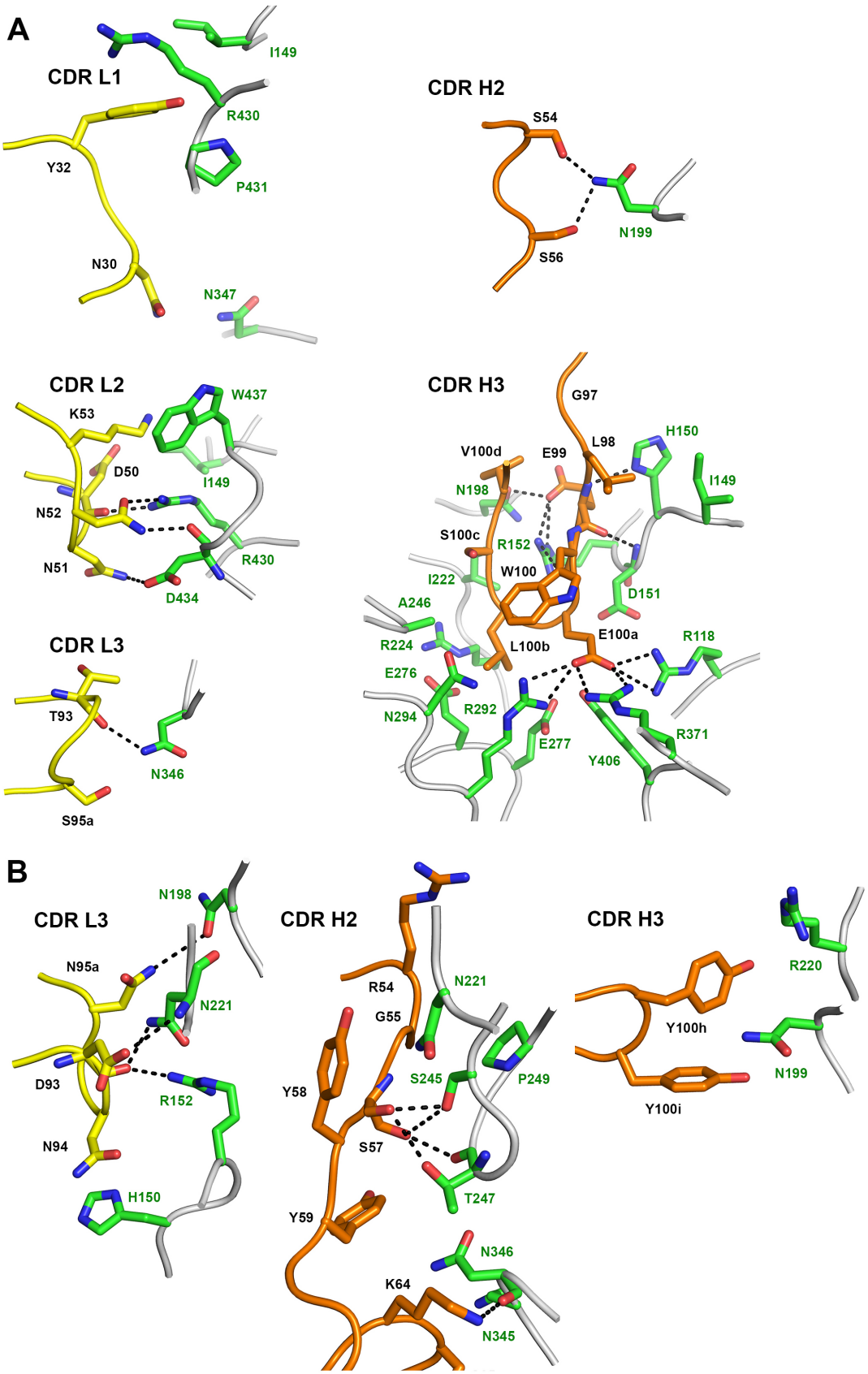
A
CDR L1
I149
R430
Y32
P431
N30
N347
CDR H2
S54
N199
S56
CDR L2
W437
K53
D50
I149
N52
R430
N51
D434
CDR H3
G97
H150
V100d
E99
L98
I149
N198
S100c
R152
W100
I222
D151
A246
E100a
R118
R224
L100b
E276
N294
R292
E277
R371
Y406
CDR L3
T93
N346
S95a
B
CDR L3
N198
N95a
N221
D93
R152
N94
H150
CDR H2
R54
N221
G55
Y58
S245
P249
S57
T247
Y59
N346
K64
N345
CDR H3
R220
Y100h
N199
Y100i

Figure S1. X-ray and cryo-EM structures of NA-45 and NA-73 Fabs with N9 NAs. Related to Figures 2, 3, 6.

(A) Interaction of Sh2 N9 Y169aH NA mutant with NA-45 Fab CDRs from the crystal structure of the Fab-NA complex at 2.3 Å resolution. NA-45 light chain is shown in yellow carbon atoms, and heavy chain in orange carbon atoms. The NA side-chains are shown in green carbon atoms. Hydrogen bonds or salt bridges are in black dotted lines.

(B) Interaction of Sh2 N9 NA with NA-73 Fab CDRs from the cryo-EM structure of the Fab-NA complex at 3.2 Å resolution. NA-73 light chain is shown in yellow carbon atoms, and heavy chain in orange carbon atoms. The NA side-chains are shown in green carbon atoms. Hydrogen bonds or salt bridges are in black dotted lines.

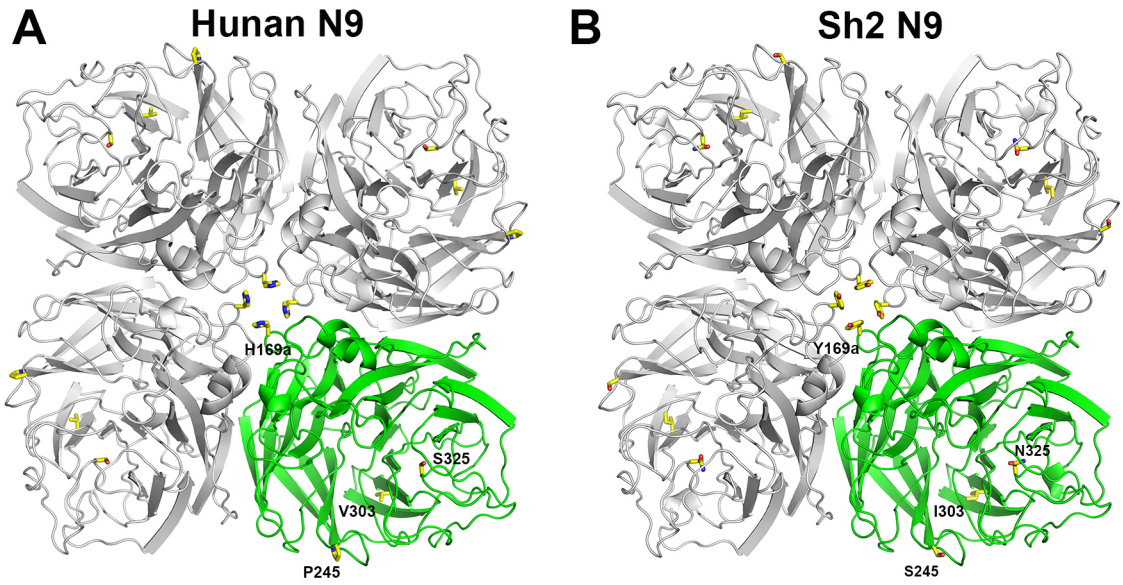

Fig. S2. Structural comparison of the NA ectodomain of Hunan N9 from its complex with NA-45 (A) and the *apo* Sh2 N9 NA (PDB code 5L14) (B). Related to Figures 1, 2, 3. The NA tetramer is viewed from above the viral surface and consists of four identical monomers in C4 symmetry. One monomer is colored in green. Four amino acid differences are found in the ectodomains of Hunan N9 and Sh2 N9 NA. The side-chains of these residues are shown in sticks.

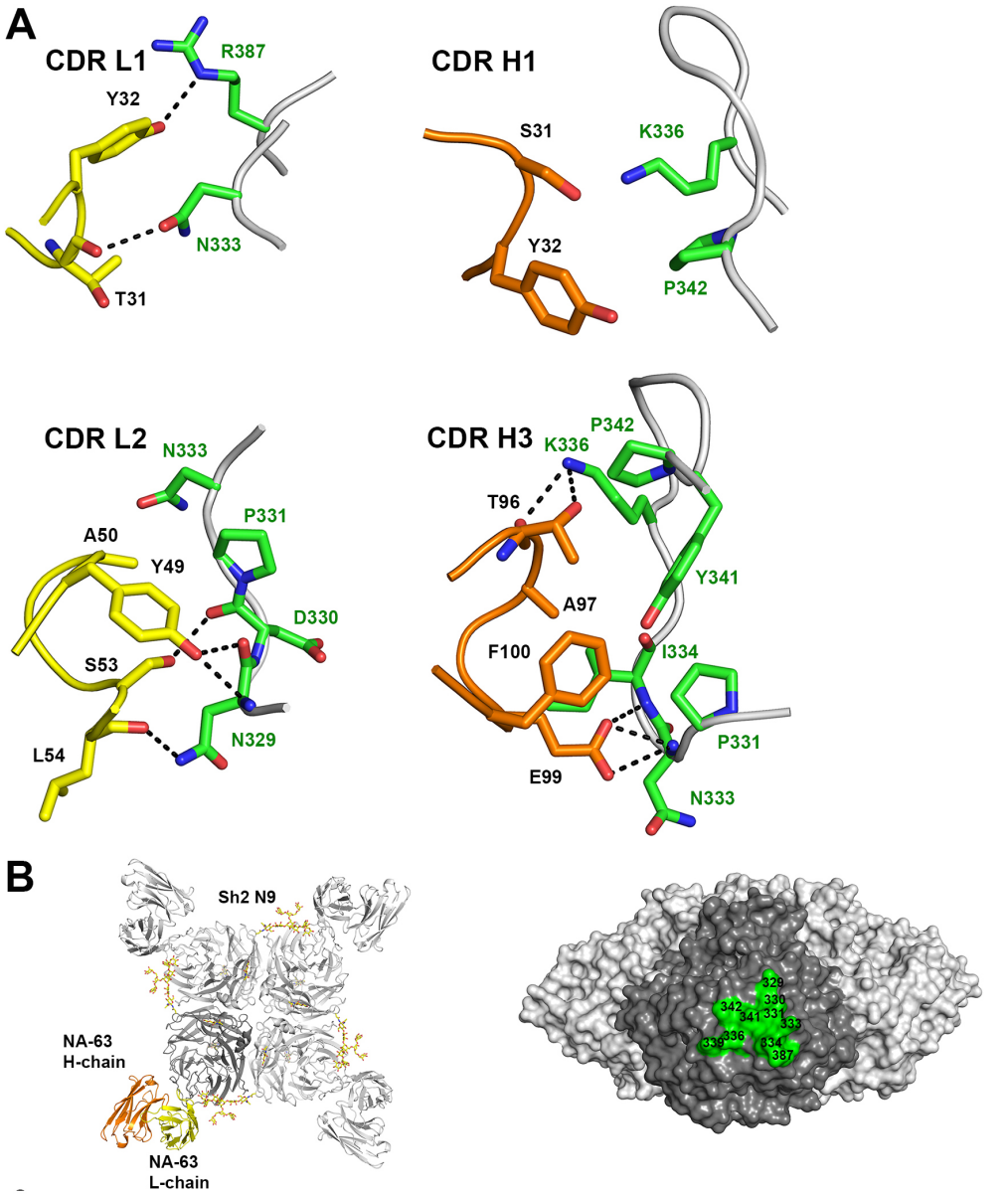
A
CDR L1
R387
Y32
N333
T31
CDR H1
S31
K336
Y32
P342
CDR L2
N333
P331
A50
Y49
D330
S53
L54
N329
CDR H3
P342
K336
T96
Y341
A97
F100
I334
P331
E99
N333
B
Sh2 N9
NA-63
H-chain
NA-63
L-chain
329
330
342
341
331
333
336
339
334
387
N329
P342
D330
Y341
P331
N333
D339
K336
I334
R387
LeuL54
SerL53
TyrL49
PheH100
AlaL50
TyrH32
ThrH96
ThrL31
SerH31
GluH99
TyrL32

Figure S3. Crystal and cryo-EM structures of NA-63 Fab with N9 NAs. Related to Figure 2.

(A) Crystal structure at 2.8 Å resolution of NA-63 with Hunan N9 NA ectodomain illustrating the Fab CDR interactions with N9 NA. The NA-63 light chain is shown in yellow carbon atoms, and heavy chain in orange carbon atoms. The side-chains of NA are shown in green carbon atoms. Hydrogen bonds or salt bridges are in black dotted lines.

(B) Cryo-EM structure of NA-63 Fab in complex with Sh2 N9 NA ectodomain plus stalk at 3.1 Å resolution. (top left) Overall structure of antibody NA-63 Fab in complex with Sh2 N9 NA. (top right) The epitope of NA-63 is mapped onto Sh2 N9 NA. (bottom) The zoomed-in molecular surface depicting the epitope of NA-63 on Sh2 N9 NA (left). The key interacting residues on NA-63 are illustrated by the antibody side chains (sticks) on a backbone ribbon on the Sh2 N9 surface NA depicting the epitope (green) (right).

A

```
          1       10        20        30        40        50        60
NA-80 VL DIVMTQSPSSLSASVGDRVTISCRASQSISSYLNWYQQKPGKAPKLLIYAASSLQSGVPS
NA-63 VL ......................T........T.......................G....
        61        70        80        90       100
NA-80 VL RFSGSASGTDFTLTISSLQPEDFATYYCQQSYSAP-FTFGPGTKVDIE
NA-63 VL .....G..........................T.LY...Q...LE.K

          1       10        20        30        40        50        59
NA-80 VH QVQLVQSGAEVKRPGASVKVSCKASGYTFISYGISWVRQAPGQGLEWMGWISAYNGNTNY
NA-63 VH E....E..GGLVQ..G.LRL..A...F..S..WM........K..D.VAN.KQDGSEKY.
        60        70        80            90       100           110
NA-80 VH AQNLQGRVTMTTDTSTSTAYMELRSLRSDDTAVYYCARVIPGTAVDYFDYWGQGTLVTVSS
NA-63 VH VDSVK..F.ISRHNAKNSL.LQMN...AE........SSTAAEFF---.............
```

B

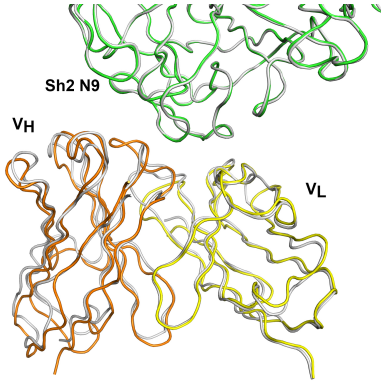

C

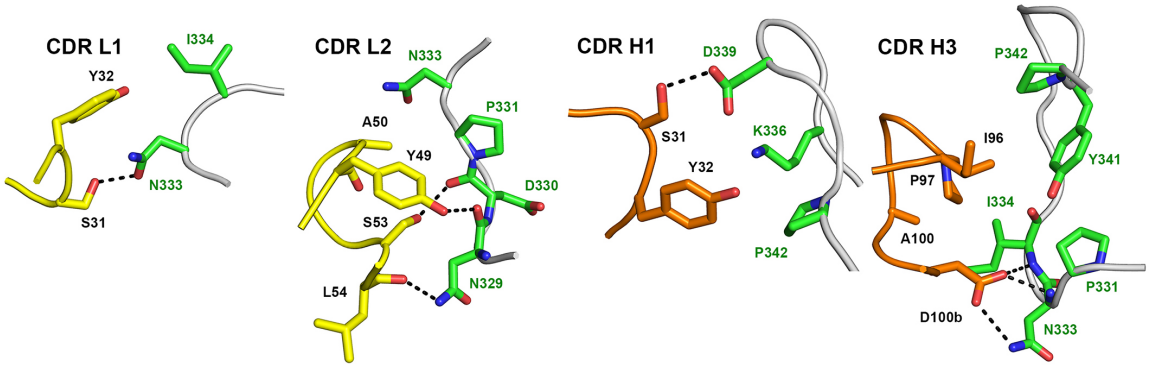

D

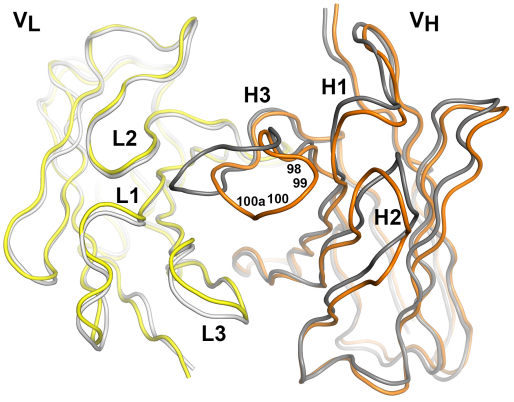

Figure S4. Cryo-EM structure of NA-80 Fab with Sh2 N9 NA at 3.6 Å resolution, angle of approach versus NA-63, and comparison of *apo* and bound NA-80 Fab. Related to Figure 2.

(A) Sequence comparison of NA-80 and NA-63 light and heavy chain variable domains with Kabat CDRs highlighted in cyan. Both antibodies use the IGKV1-39 germline, but IGHV1-18 for NA-80 and IGHV3-7 for NA-63. "-" indicates sequence deletion, "." indicates sequence identity.

(B) NA-80 and NA-63 use an almost similar angle of approach when binding to Sh2 N9 NA. Structural comparison of NA-80 Fab (yellow and orange for light and heavy chains, respectively) in complex with Sh2 N9 NA (green) with NA-63 Fab (grey) in complex with Sh2 N9 NA (grey) after superimposition of Sh2 N9 NA structures in both complexes.

(C) Interaction of the NA-80 Fab CDRs with Sh2 N9 NA. The NA-80 light chain is shown in yellow carbon atoms, and heavy chain in orange carbon atoms. The side-chains of NA are shown in green carbon atoms. Hydrogen bonds or salt bridges are in black dotted lines.

(D) Comparison of NA-80 Fab in its *apo* form (light grey and dark grey) and in its complex with Sh2 N9 NA (yellow and orange). Upon binding to Sh2 N9 NA, the CDR H3 makes large conformational changes from residues 98 to 100a.

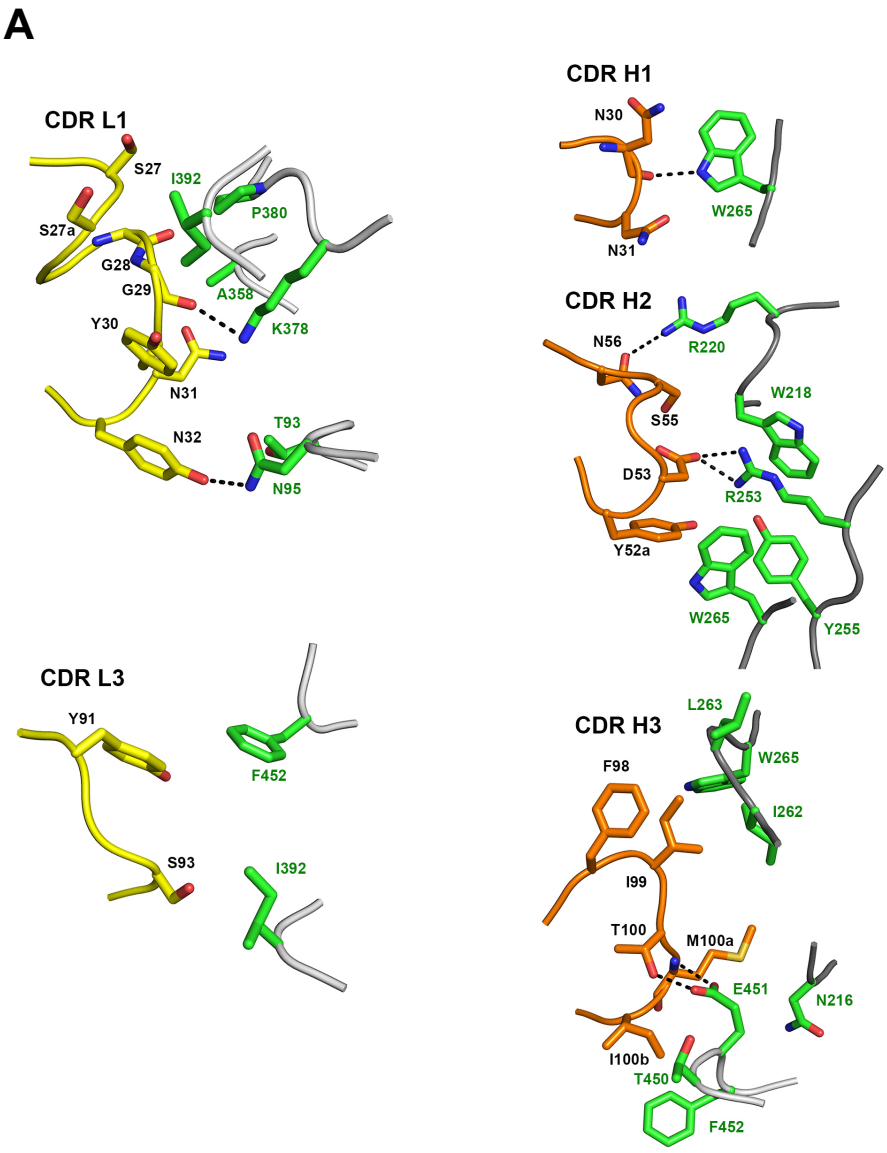
A
CDR L1
S27
I392
P380
S27a
G28
G29
A358
Y30
K378
N31
T93
N32
N95
CDR H1
N30
W265
N31
CDR H2
N56
R220
W218
S55
D53
R253
Y52a
W265
Y255
CDR L3
Y91
F452
S93
I392
CDR H3
L263
F98
W265
I262
I99
T100
M100a
E451
N216
I100b
T450
F452
B
Sh2 N9
Asn200
NA-22
L-chain
NA-22
H-chain
C
VL
VH
H1
H3
H2
L2
L1
L3

Figure S5. Cryo-EM structure of NA-22 Fab with N9 NA at 3.0 Å resolution and comparison of *apo* and bound forms. Related to Figure 2.

(A) Interaction of NA-22 Fab CDRs with Sh2 N9 NA. The NA-22 light chain is shown in yellow carbon atoms, and heavy chain in orange carbon atoms. NA-22 interacts with two NA monomers of the tetramer with one monomer shown in light grey backbone C_α atoms and the other monomer in dark grey backbone C_α atoms. The NA side-chains are shown in green carbon atoms. Hydrogen bonds or salt bridges are in black dotted lines.

(B) Structural comparison of NA-22 Fab in complex with Sh2 N9 NA (green and cyan for two adjacent protomers) with Sh2 N9 NA *apo* form (grey). Upon binding to Sh2 N9 NA, NA-22 interacts with the N-linked glycans from Asn200 of the N9 NA as indicated in highlight ellipse. The Asn200-linked glycan interacts with the adjacent N9 NA protomer in the tetramer.

(C) Comparison of NA-22 Fab in its *apo* form (light grey and dark grey) and in complex with Sh2 N9 NA (yellow and orange). No significant conformational changes of NA-22 are observed upon binding to Sh2 N9 NA.

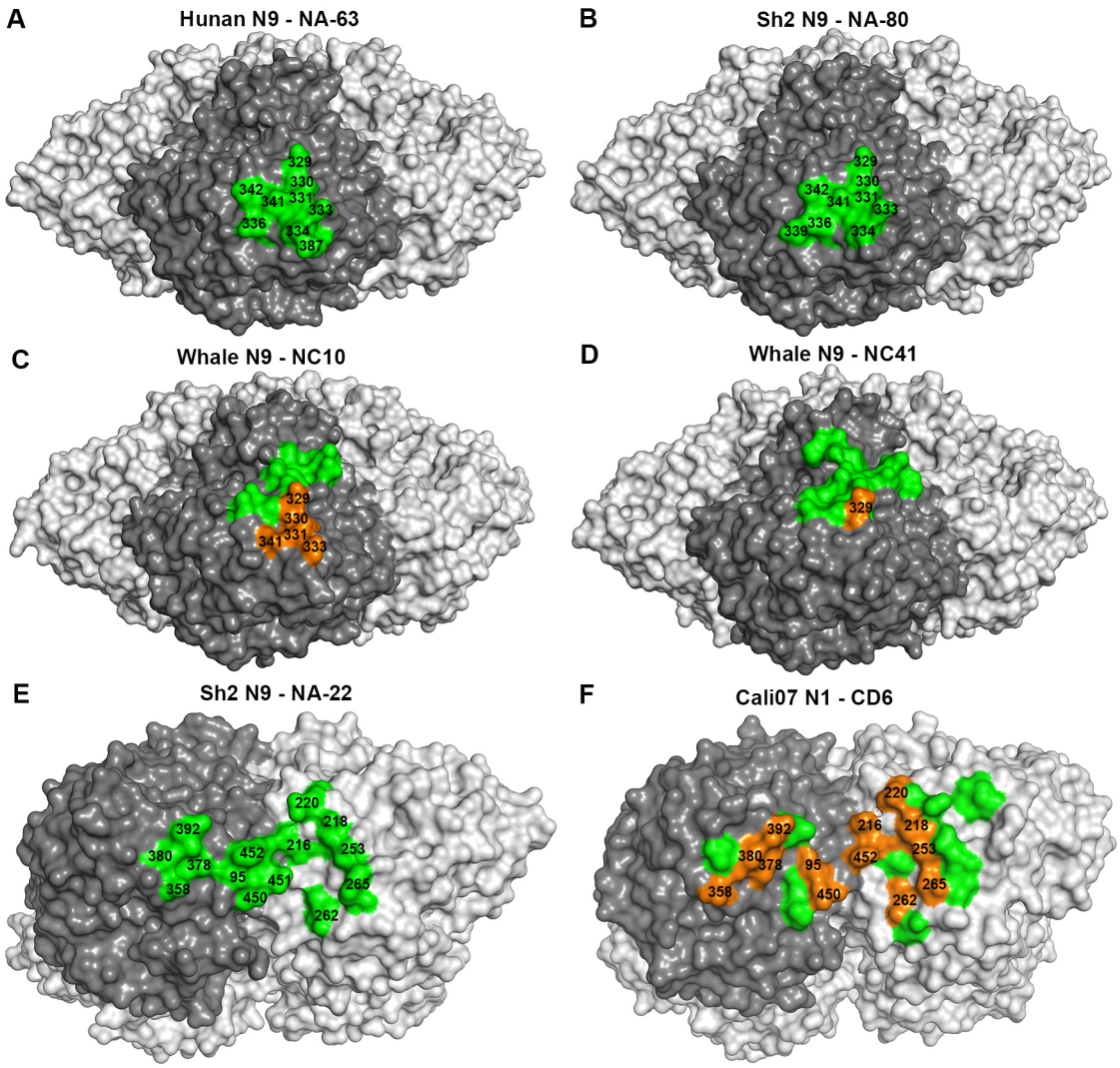

Figure S6. Epitope comparison of human antibodies NA-80, NA-63, NA-22 to Sh2 N9 NA with mouse antibodies NC10 and NC41 to whale N9 (PDB codes 1NMB and 1NCD) and mouse antibody CD6 to Cali07 N1 NA (PDB code 4QNP). Related to Figures 2 and 6.

(A) The epitope of NA-63 is mapped onto Sh2 N9 (green).

(B) The epitope of NA-80 is mapped onto Sh2 N9 (green).

(C) The epitope of NC-10 is mapped onto whale N9 (green and orange) with the overlapped epitope residues with NA-63 or NA-80 shown in orange.

(D) The epitope of NC-41 is mapped onto whale N9 (green and orange) with the overlapped epitope residues with NA-63 or NA-80 shown in orange.

(E) The epitope of NA-22 is mapped onto Sh2 N9 NA (green).

(F) The epitope of CD6 is mapped onto Cali07 N1 NA (green and orange) with the overlapping epitope residues with NA-22 shown in orange.

Table S1. Data collection and refinement statistics of crystal structures of SH2 N9 NA, NA antibodies and complexes. Related to Figures 1, 2, 3, 6.

Data set	**Sh2 N9 Y169aH**	**Sh2 N9 Y169aH NA-45 Fab**	**Hunan N9 NA-63 Fab**
Data Collection			
X-ray source	SSRL 12-2	SSRL 12-2	APS 23ID-D
Space group	I432	$P42_12$	$P42_12$
Unit cell (Å)	$a = b = c = 182.2$	$a = b = 161.3$, $c = 87.4$	$a = b = 164.6$, $c = 192.6$
Resolution (Å)[a]	43.0-1.12 (1.13-1.12)	45.8-2.30 (2.35-2.30)	49.8-2.80 (2.85-2.80)
Unique reflections	194,141	51,133	63,525
Redundancy[a]	22.3 (4.8)	6.6 (6.7)	8.4 (7.7)
Average I/σ(I)[a]	30.8 (1.1)	11.7 (2.1)	10.0 (1.0)
Completeness[a]	99.9 (97.6)	98.3 (99.2)	96.5 (78.4)
R_{sym}[a,b]	0.10 (0.92)	0.12 (0.62)	0.17 (0.98)
R_{pim}[a,b]	0.02 (0.45)	0.05 (0.26)	0.06 (0.35)
$CC_{1/2}$[a]	0.999 (0.834)	0.997 (0.962)	0.998 (0.853)
No. molecules per ASU[c]	1	1	2
Refinement			
Reflections in refinement	194,104	51,085	63,487
Refined residues	389	818	1,634
Refined waters	593	590	76
R_{cryst}[d]	0.112	0.156	0.203
R_{free}[e]	0.128	0.197	0.249
B-values (Å^2)			
Protein	11	33	77
Waters	27	36	51
Wilson *B*-values (Å^2)	7	23	59
Ramachandran values (%)[f]	96.4, 0	95.3, 0.2	94.3, 0.2
r.m.s.d. bond (Å)	0.008	0.007	0.009
r.m.s.d. angle (deg.)	1.17	0.94	1.25
PDB codes	6PZD	6PZE	6PZF

[a] Parentheses denote outer-shell statistics.
[b] $R_{sym} = \sum_{hkl}\sum_i |I_{hkl,i} - \langle I_{hkl}\rangle| / \sum_{hkl}\sum_i I_{hkl,i}$ and $R_{pim} = \sum_{hkl}[1/(N-1)]^{1/2}\sum_i |I_{hkl,i} - \langle I_{hkl}\rangle| / \sum_{hkl}\sum_i I_{hkl,i}$, where $I_{hkl,i}$ is the scaled intensity of the ith measurement of reflection *h*, *k*, *l*, $\langle I_{hkl}\rangle$ is the average intensity for that reflection, and *N* is the redundancy. $R_{pim} = \Sigma_{hkl}\,(1/(n-1))^{1/2}\,\Sigma_i\,|\,I_{hkl,i} - \langle I_{hkl}\rangle\,|\,/\,\Sigma_{hkl}\,\Sigma_i\,I_{hkl,i}$, where n is the redundancy.
[c] No. molecules for complexes refers to number of NA protomers, or NA protomers plus antibody, per asymmetric unit (ASU).
[d] $R_{cryst} = \sum_{hkl}|F_o - F_c| / \sum_{hkl}|F_o|$, where F_o and F_c are the observed and calculated structure factors.
[e] R_{free} was calculated as for R_{cryst}, but on 5% of data excluded before refinement.
[f] The values are percentage of residues in the favored and outliers regions analyzed by MolProbity (Chen et al., 2010).

Table S1. Data collection and refinement statistics - continued

Data set	**NA-80 Fab**	**NA-22 Fab**
Data Collection		
X-ray source	SSRL 9-2	SSRL 9-2
Space group	$P3_221$	$P2_12_12_1$
Unit cell (Å)	$a = b = 102.8$,	$a = 72.3$, $b = 74.5$,
	$c = 80.4$	$c = 178.3$
Resolution (Å)[a]	44.5-1.59 (1.62-1.59)	44.8-2.30 (2.34-2.30)
Unique reflections	66,498 (3,234)	43,271 (2,184)
Redundancy[a]	18.1 (7.2)	4.7 (4.4)
Average $I/\sigma(I)$[a]	58.0 (1.3)	23.4 (2.2)
Completeness[a]	99.9 (98.3)	99.3 (99.7)
R_{sym}[a,b]	0.08 (0.90)	0.08 (0.48)
R_{pim}[a,b]	0.02 (0.35)	0.04 (0.25)
$CC_{1/2}$[a]	0.999 (0.63)	0.996 (0.83)
No. molecules per ASU[c]	1	2
Refinement		
Reflections in refinement	66,460	43,207
Refined residues	451	872
Refined waters	446	341
R_{cryst}[d]	0.168	0.193
R_{free}[e]	0.204	0.236
B-values (Å^2)		
Protein	38	46
Waters	44	47
Wilson *B*-values (Å^2)	26	46
Ramachandran values (%)[f]	97.9, 0.2	96.6, 0.2
r.m.s.d. bond (Å)	0.010	0.005
r.m.s.d. angle (deg.)	1.06	0.79
PDB codes	6PZG	6PZH

[a] Parentheses denote outer-shell statistics.
[b] $R_{sym} = \sum_{hkl}\sum_i |I_{hkl,i} - \langle I_{hkl}\rangle| / \sum_{hkl}\sum_i I_{hkl,i}$ and $R_{pim} = \sum_{hkl}[1/(N-1)]^{1/2}\sum_i |I_{hkl,i} - \langle I_{hkl}\rangle| / \sum_{hkl}\sum_i I_{hkl,i}$, where $I_{hkl,i}$ is the scaled intensity of the i[th] measurement of reflection *h*, *k*, *l*, $\langle I_{hkl}\rangle$ is the average intensity for that reflection, and *N* is the redundancy. $R_{pim} = \Sigma_{hkl}\,(1/(n-1))^{1/2}\,\Sigma_i\,|\,I_{hkl,i} - \langle I_{hkl}\rangle\,|\,/\,\Sigma_{hkl}\,\Sigma_i\,I_{hkl,i}$, where n is the redundancy
[c] No. molecules for complexes refers to number of antibody Fabs per asymmetric unit (ASU).
[d] $R_{cryst} = \sum_{hkl}|F_o - F_c| / \sum_{hkl}|F_o|$, where F_o and F_c are the observed and calculated structure factors.
[e] R_{free} was calculated as for R_{cryst}, but on 5% of data excluded before refinement.
[f] The values are percentage of residues in the favored and outliers regions analyzed by MolProbity (Chen et al., 2010).

Table S2. Data collection and refinement statistics of cryo-EM structures. Related to Figures 2 and 6.

Data set	Sh2 N9 NA NA-73 Fab	Sh2 N9 NA NA-63 Fab	Sh2 N9 NA NA-80 Fab	Sh2 N9 NA NA-22 Fab
Data Collection				
Microscope	Thermo Fisher Titan Krios	Thermo Fisher Titan Krios	Thermo Fisher Titan Krios	Thermo Fisher Titan Krios
Voltage (kV)	300	300	300	300
Detector	Gatan K2 Summit	Gatan K2 Summit	Gatan K2 Summit	Gatan K2 Summit
Recording mode	Counting	Counting	Counting	Counting
Nominal magnification	29,000	29,000	29,000	29,000
Movie micrograph pixel size (Å)	1.03	1.03	1.03	1.03
Dose rate (e^-/[(camera pixel)^{2}s])	6.421	4.406	4.053	5.111
Number of frames per movie micrograph	33	48	52	42
Frame exposure time (ms)	250	250	250	250
Movie micrograph exposure time (s)	8.25	12	13	10.5
Total dose (e^-/Å^2)	50	50	50	50
Defocus range (μm)	-0.5 to -1.5	-0.5 to -1.5	-0.8 to -2.0	-1.2 to -2.0
EM data processing				
Number of movie micrographs	1,355	916	946	823
Number of molecular projection images in map	157,751	91,117	11,240	20,922
Symmetry	C4	C4	C4	C4
Map resolution (FSC 0.143; Å)	3.17	3.11	3.60	3.00
Local resolution range (Å)	2.2-3.4	2.3-3.2	2.3-6.5	2.9-3.5
Map sharpening B-factor (Å^2)	-161	-149	-112	-103
Structure building and validation				
Number of atoms in deposited model				
NA (protomer)	3,051	3,068	3,054	3,068
Fab variable region	1,801	1,733	1,752	1,742
Glycans	147	119	147	133
MolProbity score	1.05	0.80	1.05	1.19
Clash score	1.39	0.42	1.48	2.63
Map correlation coefficient	0.90	0.87	0.86	0.88
EMRinger score	4.89	4.87	4.03	5.80
r.m.s.d. bond (Å)	0.024	0.022	0.020	0.020
r.m.s.d. angle (deg.)	1.89	1.82	1.92	1.76
Ramachandran values (%)[a]	97.0, 0.3	97.2, 0.5	97.1, 0.2	97.2, 0
Side-chain rotamer outliers(%)	0	0	0	0
PDB codes	6PZY	6U02	6PZZ	6PZW

[a]Values are percentage of residues in the favored and outliers regions analyzed by MolProbity (Chen et al., 2010).

Table S3. Sequence conservation of NA-45 epitope by influenza NA subtype.

Related to Figures 2, 3, 6.

NA residue number	Sh2 N9	Hunan N9	A Group 1				A Group 2					B
			N1 (9,744)[a]	N4 (149)	N5 (237)	N8 (1,290)	N2 (12,826)	N3 (772)	N6 (1,218)	N7 (473)	N9 (587)	B NA (3,469)
118	R	R	R[b] (99.9)[c]	R (99.3)	R (99.6)	R (99.8)	R (100)	R (100)	R (100)	R (100)	R (99.8)	R (100)
149	I	I	V (54.4)	V (98.7)	V (99.6)	V (95.5)	V (65.3)	I (90.3)	I (99.2)	I (97.3)	I (99.5)	R (99.9)
150	H	H	K (99.5)	K (100)	K (99.2)	K (99.5)	H (65.9)	K (98.4)	H (99.3)	H (98.7)	H (100)	E (53.3)
151	D	D	D (99.2)	D (100)	D (99.6)	D (99.9)	D (93.5)	D (99.1)	D (99.9)	D (100)	D (99.7)	D (99.4)
152	R	R	R (100)	R (100)	R (99.6)	R (99.8)	R (99.9)	R (99.7)	R (99.8)	R (99.8)	R (99.3)	R (99.9)
198	N	N	D (99.5)	D (100)	D (99.6)	D (99.9)	D (99.6)	D (99.4)	N (97.8)	N (100)	N (99.5)	D (99.4)
199	N	N	N (81.7)	A (56.4)	D (98.7)	A (66.0)	K (59.3)	N (97.8)	N (98.1)	D (88.4)	N (99.8)	S (52.7)
222	I	I	I (99.2)	I (99.3)	I (99.6)	I (99.7)	I (99.3)	I (99.4)	I (99.3)	I (99.8)	I (100)	I (99.5)
224	R	R	R (99.9)	R (100)	R (99.2)	R (99.9)	R (99.9)	R (99.2)	R (99.5)	R (100)	R (100)	R (99.8)
246	A	A	S (99.2)	S (99.3)	A (99.6)	A (99.5)	A (99.8)	A (99.5)	A (99.5)	A (100)	A (99.5)	A (99.9)
276	E	E	E (99.9)	E (100)	E (99.6)	E (99.9)	E (99.9)	E (99.6)	E (99.6)	E (100)	E (100)	E (100)
277	E	E	E (100)	E (100)	E (99.6)	E (100)	E (100)	E (99.6)	E (99.6)	E (100)	E (100)	E (100)
292	R	R	R (99.9)	R (100)	R (99.6)	R (99.9)	R (99.9)	R (99.6)	R (99.9)	R (100)	R (98.8)	R (100)
294	N	N	N (99.8)	N (100)	N (99.2)	N (99.9)	N (99.9)	N (99.6)	N (99.8)	N (100)	N (100)	N (99.9)
346	N	N	A (98.1)	R (100)	N (99.6)	-	G (66.8)	G (88.2)	D (99.8)	A (99.6)	N (100)	-
347	N	N	N (66.2)	Y (100)	Y (100)	Y (100)	H (73.1)	P (89.5)	P (99.8)	P (99.6)	N (99.3)	G (99.7)
371	R	R	R (99.9)	R (100)	R (100)	R (100)	R (99.9)	R (100)	R (100)	R (100)	R (100)	R (99.9)
406	Y	Y	Y (99.9)	Y (100)	Y (99.6)	Y (99.9)	Y (99.9)	Y (100)	Y (100)	Y (100)	Y (100)	Y (99.9)
430	R	R	Q (100)	I (99.3)	K (98.3)	K (90.6)	R (98.8)	R (86.9)	R (98.4)	R (99.8)	R (99.1)	G (99.6)
431	P	P	P (99.3)	T (99.3)	P (99.6)	P (100)	K (69.3)	P (99.7)	P (100)	P (100)	P (100)	G (99.8)
434	D	D	N (66.7)	-[d]	R (97.0)	-	T (89.3)	N (99.5)	S (95.6)	A (99.4)	D (99.5)	-
437	W	W	I (98.6)	I (100)	I (100)	I (99.1)	W (57.6)	S (99.6)	L (99.0)	W (97.0)	W (99.5)	T (99.7)

NA residues conserved in influenza A N1 to N9 and influenza B NA are highlighted in cyan.

[a] Number of non-redundant influenza NA sequences for subtype from the Influenza Virus Resource at the National Center for Biotechnology Information (NCBI) database (https://www.ncbi.nlm.nih.gov/genomes/FLU/) in Nov 28, 2018.

[b] Most common residue at position for subtype.

[c] Percent identity for most common residue.

[d] Sequence deletion as aligned to N2 NA.

Table S4. Sequence conservation of NA-73, NA-63, NA-80, and NA-22 epitopes by influenza NA subtype. Related to Figures 2 and 6.

(A) Sequence conservation of NA-73 epitope by NA subtype.

NA residue number	Sh2 N9	Hunan N9	A Group 1				A Group 2					B
			N1 (9,744)[a]	N4 (149)	N5 (237)	N8 (1,290)	N2 (12,826)	N3 (772)	N6 (1,218)	N7 (473)	N9 (587)	B NA (3,469)
150	H	H	K[b] (99.5)[c]	K (100)	K (99.2)	K (99.5)	H (65.9)	K (98.4)	H (99.3)	H (98.7)	H (100)	E (53.3)
152	R	R	R (100)	R (100)	R (99.6)	R (99.8)	R (99.9)	R (99.7)	R (99.8)	R (99.8)	R (99.3)	R (99.9)
198	N	N	D (99.5)	D (100)	D (99.6)	D (99.9)	D (99.6)	D (99.4)	N (97.8)	N (100)	N (99.5)	D (99.4)
199	N	N	N (81.7)	A (56.4)	D (98.7)	A (66.0)	K (59.3)	N (97.8)	N (98.1)	D (88.4)	N (99.8)	S (52.7)
220	R	R	N (85.0)	G (100)	K (98.7)	G (99.7)	K (80.5)	K (74.9)	G (99.1)	G (56.4)	R (98.1)	N (51.9)
221	N	N	N (72.0)	N (100)	Q (98.7)	D (97.8)	N (50.6)	D (90.2)	N (99.6)	N (98.9)	N (99.8)	P (99.6)
245	S	P	P (99.5)	P (100)	P (99.6)	P (100)	S (89.0)	P (99.4)	P (99.4)	S (96.8)	S (92.7)	G (100)
247	T	T	N (59.7)	D (98.7)	N (92.4)	N (99.0)	S (89.7)	A (89.8)	N (99.0)	S (96.0)	T (99.7)	D (77.5)
249	P	P	Q (89.5)	Q (100)	Q (99.6)	Q (99.9)	K (73.1)	S (88.2)	R (84.5)	Q (99.6)	P (100)	D (99.4)
345	N	N	G (100)	G (100)	N (95.8)	G (98.9)	G (99.9)	G (99.6)	P (99.7)	G (98.7)	N (98.1)	D (77.5)
346	N	N	A (98.1)	R (100)	N (99.6)	-[d]	G (66.8)	G (88.2)	D (99.8)	A (99.6)	N (100)	-

(B) Sequence conservation of NA-63 epitope by NA subtype.

NA residue number	Sh2 N9	Hunan N9	A Group 1				A Group 2					B
			N1 (9,744)[a]	N4 (149)	N5 (237)	N8 (1,290)	N2 (12,826)	N3 (772)	N6 (1,218)	N7 (473)	N9 (587)	B NA (3,469)
329	N	N	N[b] (85.7)[c]	V (94.0)	Q (99.6)	E (99.6)	N (59.0)	A (80.6)	N (94.3)	S (59.0)	N (99.0)	N (72.9)
330	D	D	D (99.9)	D (100)	D (100)	D (100)	D (99.9)	D (99.6)	D (99.9)	D (100)	D (99.8)	D (100)
331	P	P	G (55.2)	G (98.7)	S (79.3)	S (75.8)	S (84.3)	P (99.6)	P (99.8)	K (98.5)	P (99.8)	G (100)
333	N	N	-[d]	-	F (100)	F (100)	S (99.8)	S (99.6)	G (47.5)	S (86.7)	N (48.9) A (27.4) T (21.8)	I (99.7)
334	I	I	T (70.9)	T (98.0)	T (83.5)	T (89.1)	S (91.2)	T (97.5)	S (56.2)	S (26.8)	V (57.9) I (41.7)	T (99.0)
336	K	K	S (83.7)	S (100)	S (100)	S (100)	H (54.0)	S (99.4)	N (96.7)	D (98.1)	K (99.3)	P (99.6)
341	Y	Y	V (93.6)	V (64.4)	V (89.0)	M (79.4)	N (99.9)	S (99.2)	I (97.6)	I (99.8)	Y (100)	G (100)
342	P	P	S (68.8)	N (100)	G (100)	G (99.9)	N (97.9)	N (89.9)	T (97.5)	T (99.6)	P (99.8)	D (77.5)
387	R	R	-	D (100)	S (100)	S (100)	N (66.3)	P (84.6)	Q (99.6)	N (95.8)	R (98.3)	D (99.4)

(C) Sequence conservation of NA-80 epitope by NA subtype.

NA residue number	Sh2 N9	Hunan N9	A Group 1				A Group 2					B
			N1 (9,744)[a]	N4 (149)	N5 (237)	N8 (1,290)	N2 (12,826)	N3 (772)	N6 (1,218)	N7 (473)	N9 (587)	B NA (3,469)
329	N	N	N[b] (85.7)[c]	V (94.0)	Q (99.6)	E (99.6)	N (59.0)	A (80.6)	N (94.3)	S (59.0)	N (99.0)	N (72.9)
330	D	D	D (99.9)	D (100)	D (100)	D (100)	D (99.9)	D (99.6)	D (99.9)	D (100)	D (99.8)	D (100)
331	P	P	G (55.2)	G (98.7)	S (79.3)	S (75.8)	S (84.3)	P (99.6)	P (99.8)	K (98.5)	P (99.8)	G (100)
333	N	N	-[d]	-	F (100)	F (100)	S (99.8)	S (99.6)	G (47.5)	S (86.7)	N (48.9) A (27.4) T (21.8)	I (99.7)
334	I	I	T (70.9)	T (98.0)	T (83.5)	T (89.1)	S (91.2)	T (97.5)	S (56.2)	S (26.8)	V (57.9) I (41.7)	T (99.0)
336	K	K	S (83.7)	S (100)	S (100)	S (100)	H (54.0)	S (99.4)	N (96.7)	D (98.1)	K (99.3)	P (99.6)
339	D	D	G (89.2)	S (66.4)	N (95.8)	S (93.9)	D (78.7)	S (94.9)	A (96.0)	N (100)	D (98.3)	S (99.5)
341	Y	Y	V (93.6)	V (64.4)	V (89.0)	M (79.5)	N (99.9)	S (99.2)	I (97.6)	I (99.8)	Y (100)	G (100)
342	P	P	S (68.8)	N (100)	G (100)	G (99.9)	N (97.9)	N (89.9)	T (97.5)	T (99.6)	P (99.8)	D (77.5)

(D) Sequence conservation of NA-22 epitope by NA subtype.

NA residue number	Sh2 N9	Huna n N9	A Group 1				A Group 2					B
			N1 (9,744)[a]	N4 (149)	N5 (237)	N8 (1,290)	N2 (12,826)	N3 (772)	N6 (1,218)	N7 (473)	N9 (587)	B NA (3,469)
95	N	N	S[b] (82.7)[c]	K (56.4)	S (99.6)	K (81.7)	T (96.1)	R (89.2)	N (99.2)	E (98.9)	N (99.8)	S (99.7)
216	N	N	K (99.5)	K (99.3)	R (99.6)	N (98.8)	G (58.5)	K (98.7)	P (50.5)	K (98.5)	N (99.5)	H (99.7)
218	W	W	W (99.9)	W (100)	W (99.6)	W (99.9)	W (99.9)	W (99.2)	W (99.5)	W (100)	W (100)	Y (99.9)
220	R	R	N (85.0)	G (100)	K (98.7)	G (99.7)	K (80.5)	K (74.9)	G (99.1)	G (56.4)	R (98.1)	N (51.9)
253	R	R	K (98.2)	K (100)	K (99.2)	R (89.7)	K (71.8)	R (99.1)	K (98.9)	K (100)	R (100)	R (99.9)
262	I	I	I (55.9)	I (99.3)	V (99.6)	I (88.4)	I (98.4)	I (72.3)	I (95.8)	V (87.7)	I (97.8)	I (99.7)
265	W	W	S (99.0)	M (56.4)	E (99.6)	Q (96.9)	I (54.6)	Y (95.7)	I (91.7)	E (100)	W (100)	E (99.9)
358	A	A	N (98.4)	D (99.3)	N (84.8)	N (70.9)	N (85.6)	N (84.6)	E (49.9)	D (46.5)	G (41.6) A (34.9) V (15.5)	I (99.3)
378	K	K	W (99.9)	W (100)	L (96.6)	K (79.0)	K (76.6)	K (99.1)	K (98.9)	K (99.8)	K (99.8)	V (99.6)
380	P	P	P (99.8)	A (100)	E (99.6)	R (78.8)	I (74.2)	T (88.7)	P (100)	P (99.8)	P (100)	Y (100)
392	I	I	S (98.4)	N (100)	V (63.7)	I (87.3)	I (59.8)	S (88.6)	V (47.5)	T (58.6)	I (49.9) T (49.6)	A (92.7)
450	T	T	N (89.5)	N (87.2)	S (99.2)	D (98.0)	S (99.7)	D (99.1)	K (73.4)	P (100)	T (99.3)	G (100)
451	E	E	S (94.9)	S (100)	S (98.3)	H (79.7)	G (99.8)	N (100)	E (99.7)	I (39.3)	E (99.8)	S (99.8)
452	F	F	D (80.3)	D (100)	E (99.2)	E (85.9)	T (99.8)	E (99.9)	R (99.4)	S (51.0)	F (99.8)	G (99.7)

NA residues conserved in influenza A N1 to N9 and Influenza B NA are highlighted in cyan**.** NA residues not conserved in Sh2N9 and Hunan N9 is highlighted in yellow.

[a] Number of non-redundant influenza NA sequences for subtype from the Influenza Virus Resource at the National Center for Biotechnology Information (NCBI) database (https://www.ncbi.nlm.nih.gov/genomes/FLU/) in Nov 28, 2018.

[b] Most common residue at position for subtype.

[c] Percent identity for most common residue.

[d] Sequence deletion as aligned to N2 NA.

Table S5. Oligonucleotides used in this study. Related to Key Resources Table.

REAGENT or RESOURCE	SOURCE	IDENTIFIER
NA-22-VH-F: GGT TCC ACT GGT GAC CAG GTG CAG CTG GTG GAG TCT	Integrated DNA Technologies	N/A
NA-22-VH-R: TCC CTT AGT AGA AGC TGA GGA GAC GGT GAC CAG GG	Integrated DNA Technologies	N/A
NA-22-VL-F: GGT TCC ACT GGT GAC CAG TCT GTG CTG ACT CAG CCT GC	Integrated DNA Technologies	N/A
NA-22-VL-R: AGC CTT TGG TTG TCC TAG GAC GGT GAC CTT GGT CCC	Integrated DNA Technologies	N/A
NA-45-VH-F: GGT TCC ACT GGT GAC CAG GTG CAG CTG GTG GAG TCG	Integrated DNA Technologies	N/A
NA-45-VH-R: TCC CTT AGT AGA AGC TGA GGA GAC GGT GAC CAG GG	Integrated DNA Technologies	N/A
NA-45-VL-F: GGT TCC ACT GGT GAC CAG TCT GTG CTG ACT CAG CCG C	Integrated DNA Technologies	N/A
NA-45-VL-R: AGC CTT TGG TTG TCC TAG GAC GGT GAC CTT GGT CCC	Integrated DNA Technologies	N/A
NA-63-VH-F: GGT TCC ACT GGT GAC GAG GTG CAG CTG GTG GAG TCT G	Integrated DNA Technologies	N/A
NA-63-VH-R: TCC CTT AGT AGA AGC TGA GGA GAC GGT GAC CAG GG	Integrated DNA Technologies	N/A
NA-63-VL-F: GGT TCC ACT GGT GAC GAC ATT GTG ATG ACT CAG TCT CCA TCC	Integrated DNA Technologies	N/A
NA-63-VL-R: AGC GGC CAC CGT ACG TTT GAT CTC CAG CTT GGT CCC C	Integrated DNA Technologies	N/A
NA-80-VH-F: GGT TCC ACT GGT GAC CAG GTT CAG CTG GTG CAG TCT G	Integrated DNA Technologies	N/A
NA-80-VH-R: TCC CTT AGT AGA AGC TGA GGA GAC GGT GAC CAG GG	Integrated DNA Technologies	N/A
NA-80-VL-F: GGT TCC ACT GGT GAC GAC ATT GTG ATG ACC CAG TCT CCA	Integrated DNA Technologies	N/A
NA-80-VL-R: AGC GGC CAC CGT ACG TTC GAT ATC CAC TTT GGT CCC AGG	Integrated DNA Technologies	N/A

NA-73-F: AGC CTT TGG TTG TCC TAG GAC GGT CAG CTT GGT CCC	Integrated DNA Technologies	N/A
NA-73-R: TCC CTT AGT AGA AGC TGA GGA GAC GGT GAC CAG GG	Integrated DNA Technologies	N/A
Sh2N9ect-F: CTA GCT AGT CTA GAA GGA ATT TCA ATA ACT TAA CTA AAG GGC TCT GT	Integrated DNA Technologies	N/A
Sh2N9ect-R: GGA CTG GAA AGC TTT TAG AGG AAG TAC TCT ATT TTA GCC CCA TCA	Integrated DNA Technologies	N/A
Sh2N9stalk-F: CTA GCT AGT CTA GAC TAA AAC CGG GCT GCA ATT GC	Integrated DNA Technologies	N/A
Sh2N9stalk-R: GGA CTG GAA AGC TTT TAG AGG AAG TAC TCT ATT TTA GCC CCA TCA	Integrated DNA Technologies	N/A
Sh2N9-Y169aH-F: CAC AGT GCA CAA CAG CAG GGT GGA ATG CA	Integrated DNA Technologies	N/A
Sh2N9-Y169aH-R: CTG TTG TGC ACT GTG GGC GGT GATGAT AGT G	Integrated DNA Technologies	N/A
HunanN9ect-F: CTA GCT AGT CTA GAA GGA ATT TCA ATA ACT TAA CTA AAG GGC TCT GT	Integrated DNA Technologies	N/A
HunanN9ect-R: GGA CTG GAA AGC TTT TAG AGG AAG TAC TCT ATT TTA GCC CCA TCA	Integrated DNA Technologies	N/A